GCAGS JOURNAL
A Publication of the Gulf Coast Association of Geological Societies
www.gcags.org

Upper Cretaceous (Campanian) Ozan and Annona Chalks in Caddo–Pine Island Field, Northwestern Louisiana: Depositional Setting, Lithofacies, and Nanopore/Micropore Network

Robert G. Loucks, Gregory Frébourg, and Harry D. Rowe

Bureau of Economic Geology, Jackson School of Geosciences, University of Texas at Austin, University Station, Box X, Austin, Texas 78713–8924, U.S.A.

ABSTRACT

The Caddo–Pine Island Field is a very old, shallowly buried (<2000 ft; <600 m) producing field that was discovered in 1905. One of its main reservoirs is the tight Annona Chalk, which is presently produced by the fracking of horizontal wells. A long (~200 ft [~60 m]), vertical core recovered from the Ozan Chalk and Annona Chalk sections has been analyzed to understand under what conditions the chalks were deposited and what mineralogic and diagenetic processes produced chalks with fair to very good porosity (Ozan arithmetic mean = 17.4%; Annona arithmetic mean = 23.8%) but poor permeability (Ozan arithmetic mean = 0.18 md; Annona arithmetic mean = 0.42 md). The chalks are classified as chalky marls having more than 5% clay. The Campanian Annona Chalk and Ozan Chalk were deposited during a second-order sea-level rise on the drowned Lower Cretaceous constructed platform. Depositional setting for these chalks is interpreted as deeper shelf, distal from any siliciclastic source, below storm-wave base, and in a low-energy and well-oxygenated bottom environment. Several cycles of covariant calcite and clay-mineral content suggest changes in either sea level or climate or a combination of both. The relatively small amount of clay is important because it enhanced compaction and cementation, which are the two main diagenetic processes reducing reservoir quality. The pore network is composed of interparticle and intraparticle nano- to micropores. The submicron pore throats between the coccolith platelets and clay are responsible for the low permeabilities. With advanced drilling and completion technologies and an estimated 94% of in-place reserves remaining, the shallowly buried Annona Chalk will be of continued economic interest. With a future increase in oil prices, even the Ozan Chalk may become of interest as an oil target.

INTRODUCTION

The Caddo–Pine Island Field (Fig. 1) is a very old producing field (oil) that was discovered in 1905 (Sartor, 2003). One of its main reservoirs is the shallowly buried (<2000 ft; <600 m) Upper Cretaceous Annona Chalk (Fig. 2). Much work has been done on the paleontology of this formation (e.g., Thomas and Rice, 1932; Crane, 1965; Bottjer, 1981, 1985), but nearly nothing has been completed on its depositional systems (e.g., Bottjer, 1981), especially the lithofacies and pore networks. Therefore, the major goal of this study is to define the depositional setting, lithofacies, and pore networks of the Annona Chalk and Ozan Chalk in the Caddo–Pine Island Field. Specific objectives are to: (1) review the regional geologic setting; (2) define the lithofacies of the chalks based on core, thin-section, paleontology, scanning electron microscopy (SEM), X–ray diffraction (XRD), and X–ray fluorescence (XRF) data; (3) provide a depositional model based on lithofacies; (4) describe pore types and the pore network; and (5) define the reservoir quality based on porosity, permeability, and mercury-injection capillary-pressure (MICP) analyses. The study of these more shallowly buried chalks is important because they have higher porosities and matrix permeabilities than the more deeply buried Upper Cretaceous Buda and Austin chalks. The shallowly buried Annona Chalk reservoir may be an analog for possible, yet undiscovered shallowly buried Buda and Austin chalks in the onshore Gulf of Mexico.

Manuscript received February 23, 2017; revised manuscript received May 11, 2017; manuscript accepted May 26, 2017.

GCAGS Journal, v. 6 (2017), p. 73–91.

METHODS AND DATA

Rock data for this investigation comes from a core taken in 1962 from the Thrash (Pan American Petroleum) J. J. Jolly Heirs No. 1 well at the Caddo–Pine Island Field in Caddo Parish, Louisiana (Figs. 1, 3, and 4). As shown in Figures 3 and 4, coring

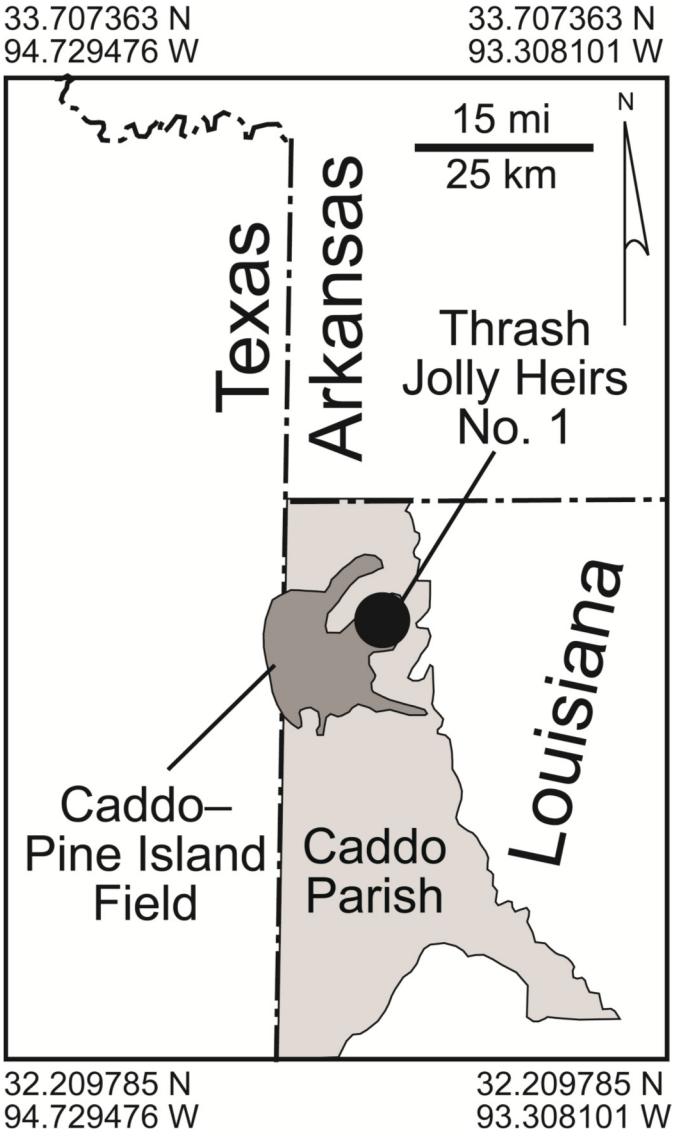

Figure 1. Locations of the Caddo–Pine Island Field and the Thrash Jolly Heirs No. 1 core.

started in the Marlbrook Marl at 1630 ft (497 m), continued through the Annona Chalk with a few coring breaks, and recovered much of the Ozan Chalk down to 1830 ft (558 m). The well did not penetrate the base of the Ozan Chalk. Out of the 200 ft (61 m) cored section, 158 ft (48 m) of core were recovered. The cores were slabbed and etched with diluted HCl acid, a treatment that cleans the face of the core and brings out greater detail. It also causes less-soluble minerals such as dolomite, quartz, and clay to stand in relief, making their identification much easier. The cores were described using a binocular microscope. The carbonate-texture classification of Dunham (1962) was used to classify the carbonate rocks. Fabric, texture, biota type and abundance, depositional features, bioturbation, and mineralogy were recorded. The wireline log for the cored section is shown in Figure 3. Twenty-four polished thin sections were prepared. The thin sections were impregnated with blue-dyed epoxy to emphasize macropores (rare) and with blue-fluorescent epoxy to emphasize micropores (common). The thin sections were described using a petrographic microscope. Thin-section texture, fabric, biota, mineralogy, diagenetic features, and visible pore types were recorded.

Because many diagenetic features and pores can only be resolved at the nano- to microscale, samples were observed using

Age (M.Y.)		Series	Stage	Group	Formation
66	Upper Cretaceous	Gulfian	Maastrichtian	Navarro	
					Saratoga
72.1			Campanian	Tayor	Marlbrook
					Annona
					Ozan
83.6			Santonian	Austin	Brownstown
86.3					

Figure 2. Stratigraphic section in the area of investigation. Adapted from Cushing et al. (1964) and Johnston et al. (2000).

an FEI Nova NanoSEM 430 at the University of Texas at Austin. Use of this field-emission SEM (FESEM) equipped with in-lens secondary electron detectors provided greatly enhanced detail of nanometer-scale features. Lower accelerating voltages (10–15 kV) were generally used on these samples to prevent beam damage; working distances were 3 to 7 mm. Two types of samples were viewed with the SEM: rock chips and Ar–ion milled samples. Rock chips allow the simple three-dimensional (3D) aspect of the grains to be observed but are not good for viewing pore networks or for detailing relationships along a single plane. Ar–ion milled samples (see Loucks et al., 2009, for discussion of description and preparation of Ar–ion milled samples) are excellent for observing flat surfaces without any irregularities related to differential hardness but allow limited 3D viewing because they are not impregnated with epoxy. The spatial distribution of nano- and micropore networks can be observed and defined at the appropriate resolution.

Semi-quantitative XRD analysis was conducted on 48 samples for mineralogy; the results are displayed in Figure 5. Samples were collected at approximately 3 ft (1 m) intervals. A rotary drill bit was used to collect samples on the back of the core, and the surface material was discarded. The sample was sieved through a 150 µm mesh screen. Approximately 15 mg of each powder sample was analyzed using an InXitu BTX 308 Portable XRD Analyzer at the University of Texas at Austin. Bulk geochemical data were collected from the cores utilizing dispersive XRF with a Bruker handheld energy-dispersive XRF analyzer. The analyzer was connected to and controlled by laptop computers during acquisition. The spectrometers are capable of analyzing major and trace elements by performing two separate analyses. For this study, only Ca, Al, and Ti were used to define marine- versus terrigenous-sourced sediment. The cores were scanned at a 1 ft (0.3 m) interval.

Porosity and permeability measurements were conducted on 15 core plugs (1 in [2.5 cm] diameter) by Weatherford Laboratories. Samples were not stressed, and permeabilities are Klinkenberg corrected. MICP analyses were run on two samples, one each from the Annona Chalk and the Ozan Chalk, by Weatherford Laboratories. The samples were subjected to 60,000 psi (414 MPa) to ensure accurate measurement of micropore throats.

REGIONAL DEPOSITIONAL SETTING AND GENERAL STRATIGRAPHY

Following Lower Cretaceous deposition, a major second-order sea-level rise drowned the shelf in the northern Gulf of Mexico (Phelps et al., 2014) (Fig. 6). In the area of northern Louisiana, sedimentation took place on this drowned Lower Cretaceous shelf during the Campanian. Following the siliciclastic Del Rio Clay deposition (Cenomanian) over the drowned Lower Cretaceous shelf, a series of chalks were deposited (Fig. 2). The

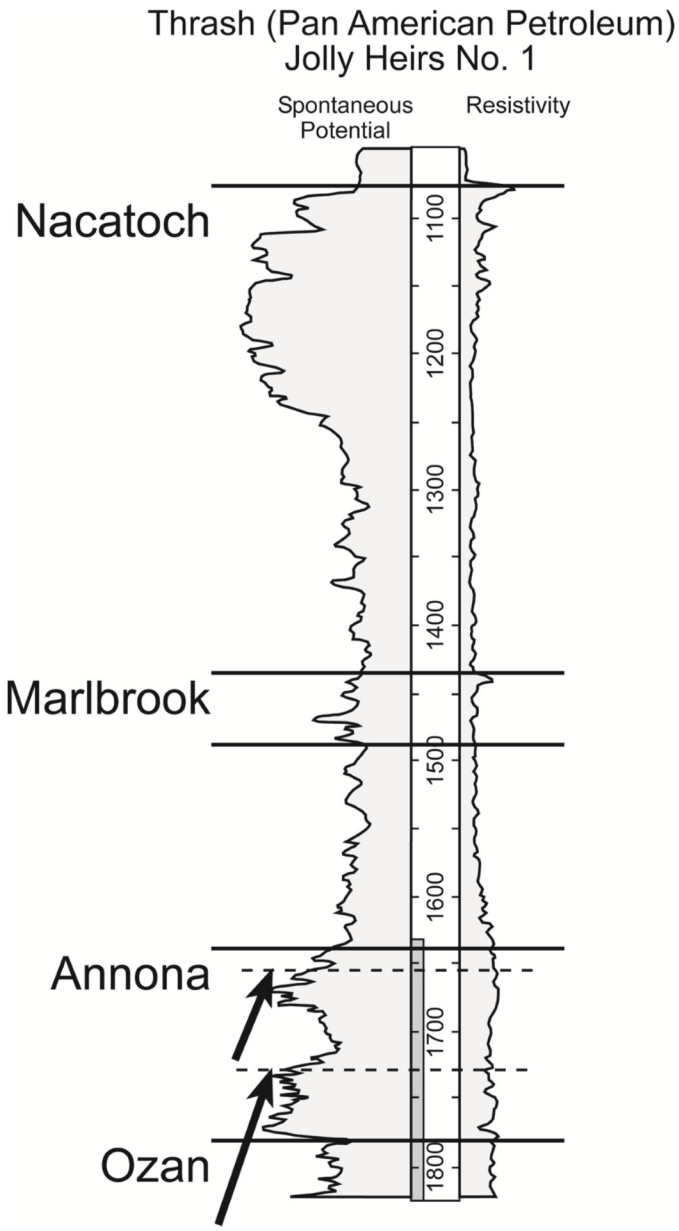

Figure 3. Thrash Jolly Heirs No. 1 wireline log. Gray bar shows cored interval. Arrows show clay-mineral/calcite cycles.

oldest was the Buda chalk, followed by the argillaceous Eagle Ford and Austin chalks (stratigraphic section ranged from the Cenomanian to the Santonian). During the Campanian, four chalk units were deposited in the northern Louisiana area, the Ozan, Annona, Marlbrook, and Saratoga (Crane, 1965) (Fig. 2). The stratigraphic pick between the Ozan and Annona units are based on correlations shown in the type log for the Caddo–Pine Island Field (see figure 9 of Sartor [2003]). On the basis of paleontology, Bottjer (1985) documented an unconformity between the Ozan Chalk and Annona Chalk. Cushing et al. (1964) mentioned that the Ozan reaches up to 200 ft (60 m) thick in southwestern Arkansas and the Annona reaches up to 400 ft (122 m) thick in Louisiana and Texas. As mentioned, the core used in the present study sampled several feet of Marlbrook Chalk, the full Annona Chalk section, and most of the Ozan Chalk.

The paleogeographic map of North America for the period around 75 Ma shows the Annona and Ozan chalks deposited on a downed shelf (Fig. 6). The Western Interior Seaway was open to the north allowing an exchange of colder waters from the far north with the warmer waters of the Gulf of Mexico. In this area of the Gulf of Mexico, the shelf was approximately 300 mi (483 km) wide. The large eastern North American land mass was situated approximately 100 mi (160 km) north of the Caddo–Pine Island Field, and the deep Gulf of Mexico was situated approximately 200 mi (320 km) to the south.

Deposition in the area of investigation would have been relatively deepwater open marine (below storm-wave base), away from terrigenous input, and well oxygenated. Lateral continuity of lithofacies should be high (tens of miles) because the depositional processes would have been uniform over broad areas of the deeper shelf and the sediment homogenized by bioturbation.

LITHOFACIES AND MINERALOGY

The lithofacies of the Ozan Chalk and Annona Chalk are relatively simple, generally a combination of calcite and siliciclastic mud (Fig. 5). Minor amounts of phosphate are scattered throughout the section. All of the sediments were intensely bioturbated. Bottjer (1985) reported on Ozan and Annona trace fossils and recognized *Planolites*, *Chondrites*, *Thalassinoides*, and *Zoophycos*.

Mineralogy

Figure 5 shows the general mineralogy in the cored section to be predominantly calcite, with siliciclastic material ranging from 3% to 20% and one outlier at 38%. According to Longman et al. (1998), coccolith-dominated limestones with less than 5% siliciclastic material are pure chalks, and samples with 5% to 50% siliciclastic material are chalky marls. The limestone samples in this investigation would be classified as predominantly chalky marls by Longman et al. (1998). The siliciclastic mud is a mixture of clay-sized quartz and clay minerals (Bottjer, 1981), with a greater abundance of quartz than of clay. The clay is predominantly smectite, as would be expected with the shallow depth of burial of the Ozan and Annona sections (<2000 ft [<600 m]).

The samples from the Ozan Chalk are all chalky marl, with quartz averaging between 8% and 20% and clay minerals from 2% to 6%. Calcite ranges between 78% and 90%. The Annona Chalk samples are nearly all chalky marls, with a few being pure chalk. Calcite ranges between 79% and 96%, quartz between 4% and 11%, and clay between 1% and 11%. One Annona sample is rich in clay and quartz. The two analyzed Marlbrook samples plot at the calcite-rich area of the chalky marls, averaging about 90% calcite (Fig. 5); the wireline log indicates that most of the section is argillaceous (Fig. 3).

Lithofacies

Ozan Chalk (Fig. 7)

The Ozan Chalk is predominantly composed of planktic foraminifer chalky marl with an argillaceous coccolith matrix. Using the carbonate-texture classification of Dunham (1962), the Ozan Chalk would be a skeletal lime wackestone with a few units of skeletal lime mud-dominated packstone (Fig. 4). Fossils include globigerinids, benthic foraminifers, coccoliths, echinoderm fragments, ostracods, and bivalve fragments (Fig. 7). Visible allochems in thin section range from 20% to 40%. The Ozan Chalk has a rich assemblage of planktic foraminifers (e.g., Figs. 7D and 7E). In thin section, the matrix appears to have a compacted peloidal texture (Fig. 7D), which may either be marine-snow aggregates or peloids. Burrows are predominantly *Planolites* and *Chondrites*. Hardgrounds are common in chalks (e.g., Kennedy and Garrison, 1975) (Fig. 7A), and eroded hardground clasts are noted at 1829 ft (557 m). At 1793 ft (547 m) in the core are transported lime mud clasts (Fig. 7D) representing a debris flow that appears to have been activated updip.

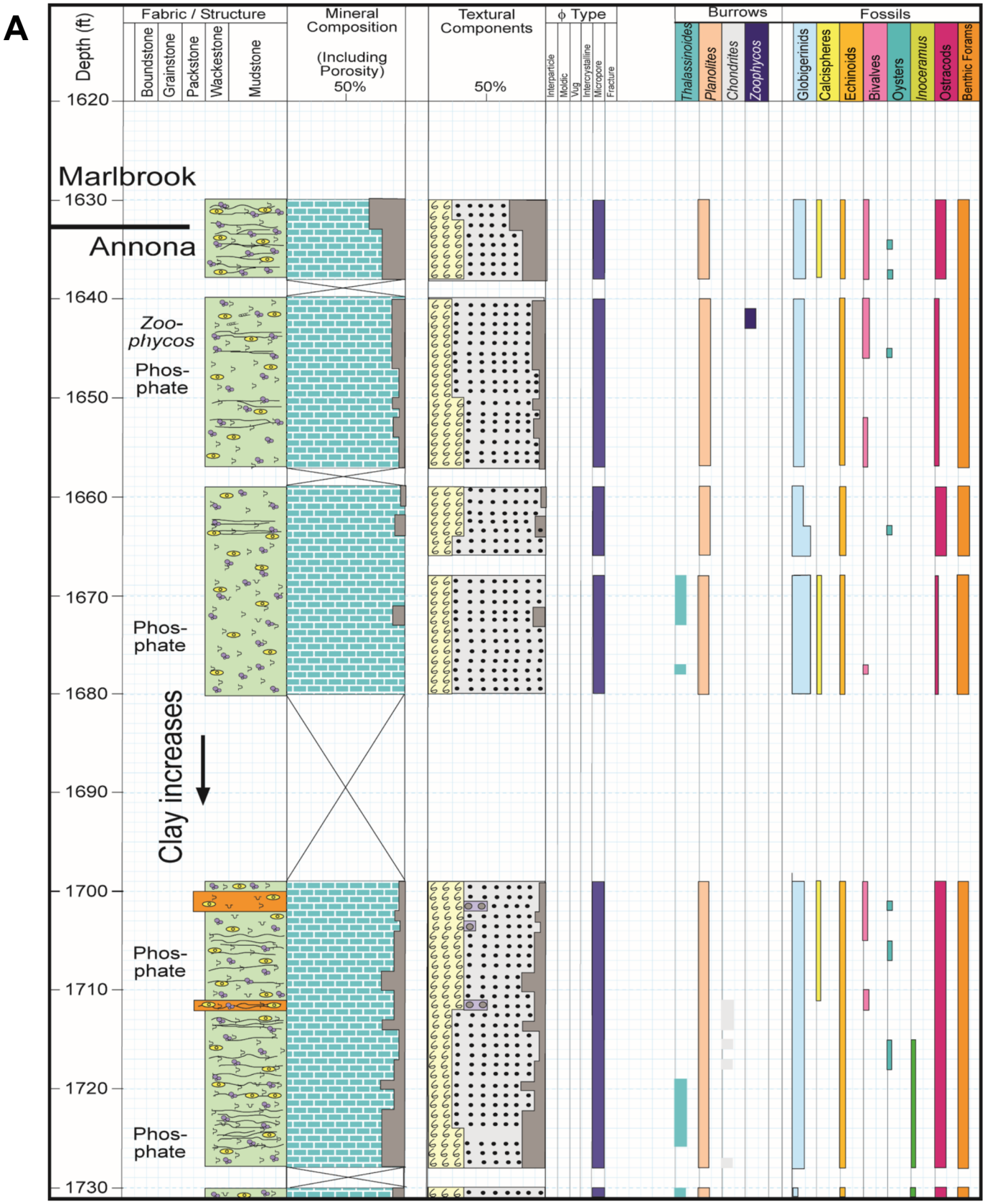

Figure 4. Core description of the Thrash Jolly Heirs No. 1. (A, ABOVE) 1630–1731 ft. (B, FACING PAGE) 1730–1830 ft. (C, FACING PAGE) Legend.

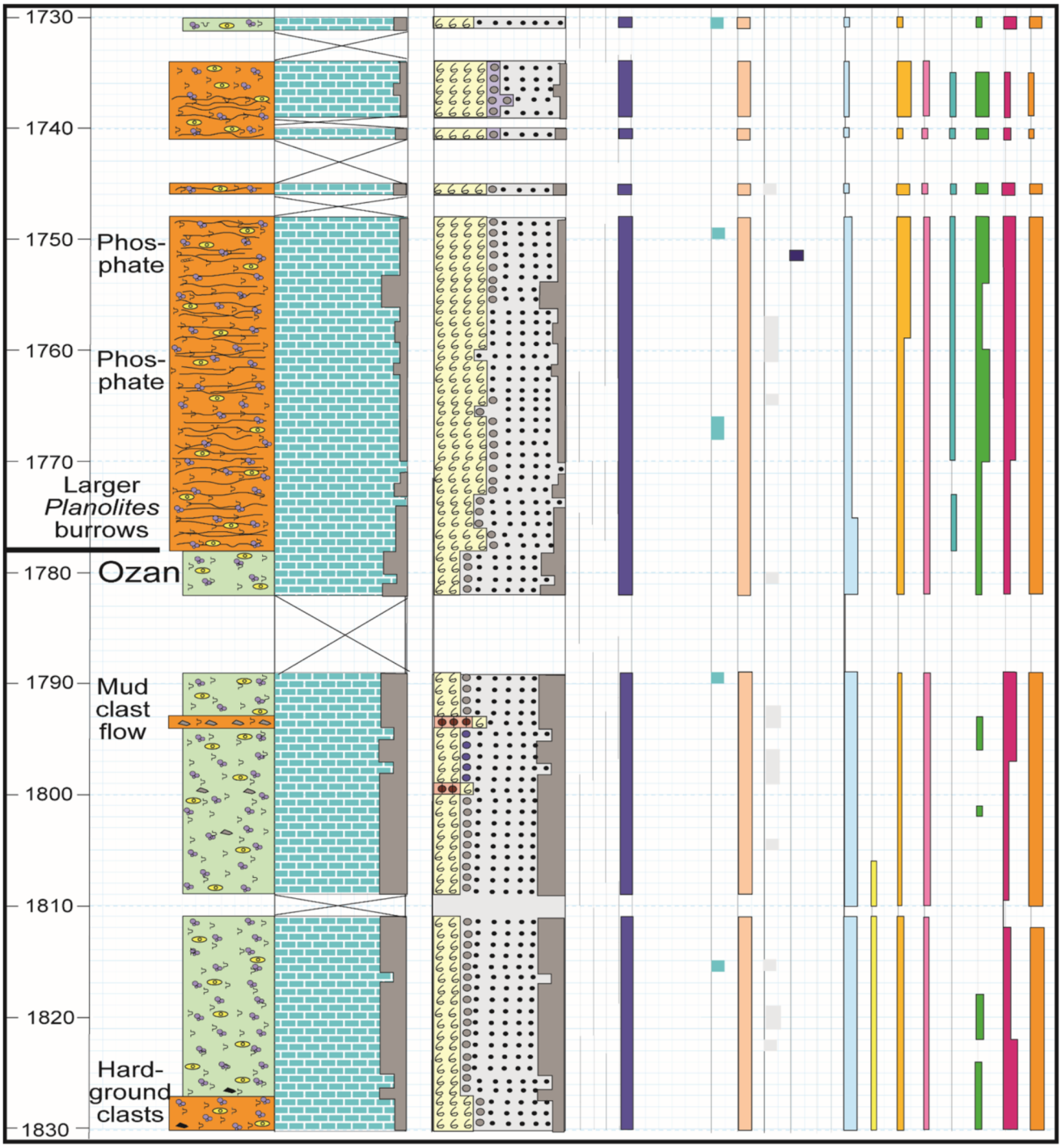

Figure 4. Core description of the Thrash Jolly Heirs No. 1. (A, FACING PAGE) 1630–1731 ft. (B, ABOVE) 1730–1830 ft. (C, LEFT) Legend.

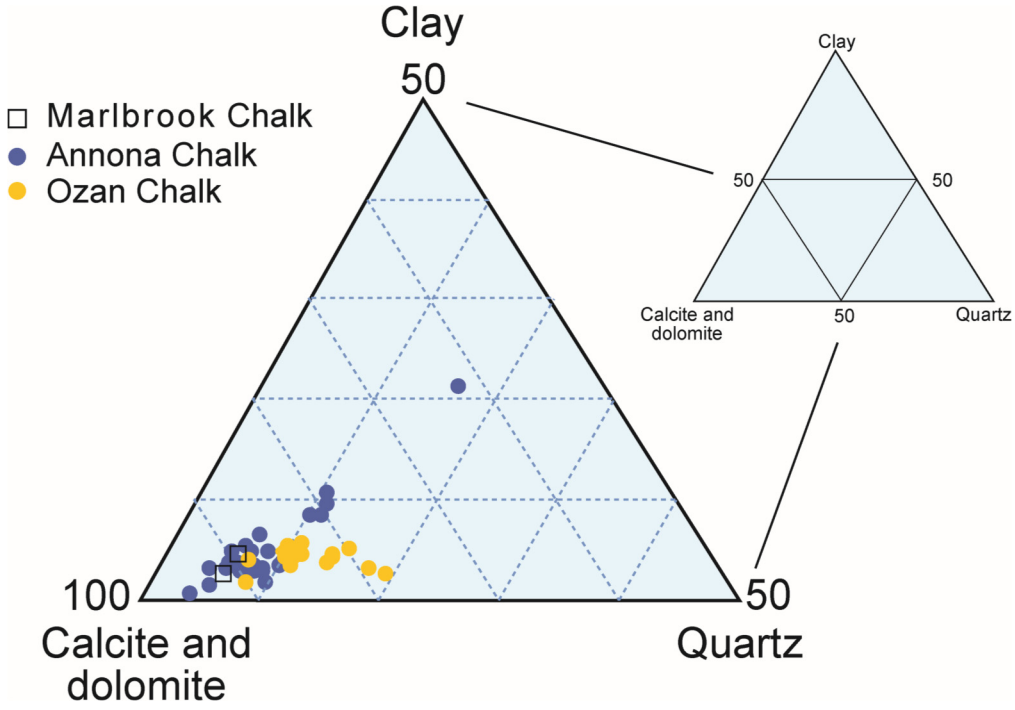

Figure 5. Ternary mineral diagram based on XRD data.

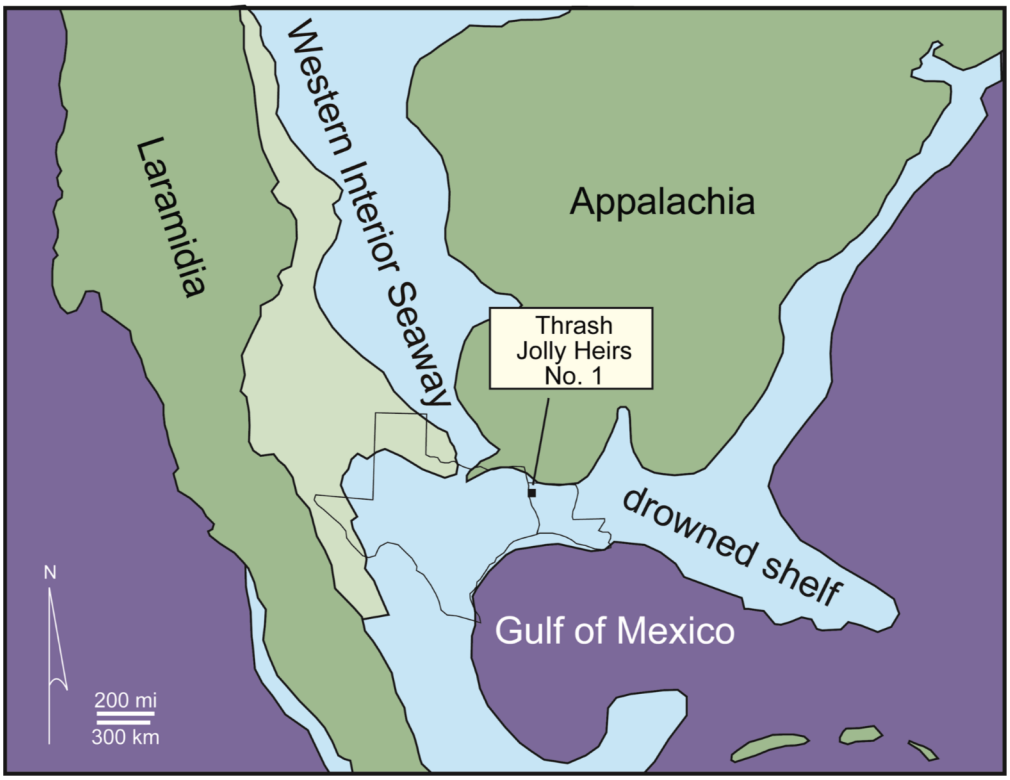

Figure 6. Simplified Campanian paleogeographic map of North America showing the regional drowned-shelf area along the northern Gulf of Mexico. General land masses modified after Blakey (2016).

Annona Chalk (Figs. 8 and 9)

The Annona Chalk, like the Ozan Chalk, is predominantly composed of planktic foraminifer chalky marl. According to the Dunham (1962) classification, the samples would be skeletal lime wackestones and skeletal lime mud-dominated packstones. The lower half of the Annona Chalk is packstone and the upper half is wackestone (Fig. 4). Fossils are similar to those of the Ozan Chalk, except the Annona contains some oyster fragments (*Ostrea* sp.) (Fig. 8D). Visible allochems in thin section range from 20% to 50%. The matrix is composed of coccoliths (Fig. 9) (Bottjer, 1981) and compacted peloids (Fig. 8E). *Planolites* (Fig. 8B) and *Chondrites* are the dominant burrows, but a few zones of *Thalassinoides* (Fig. 8A) are present, as well as some possible traces of *Zoophycos*.

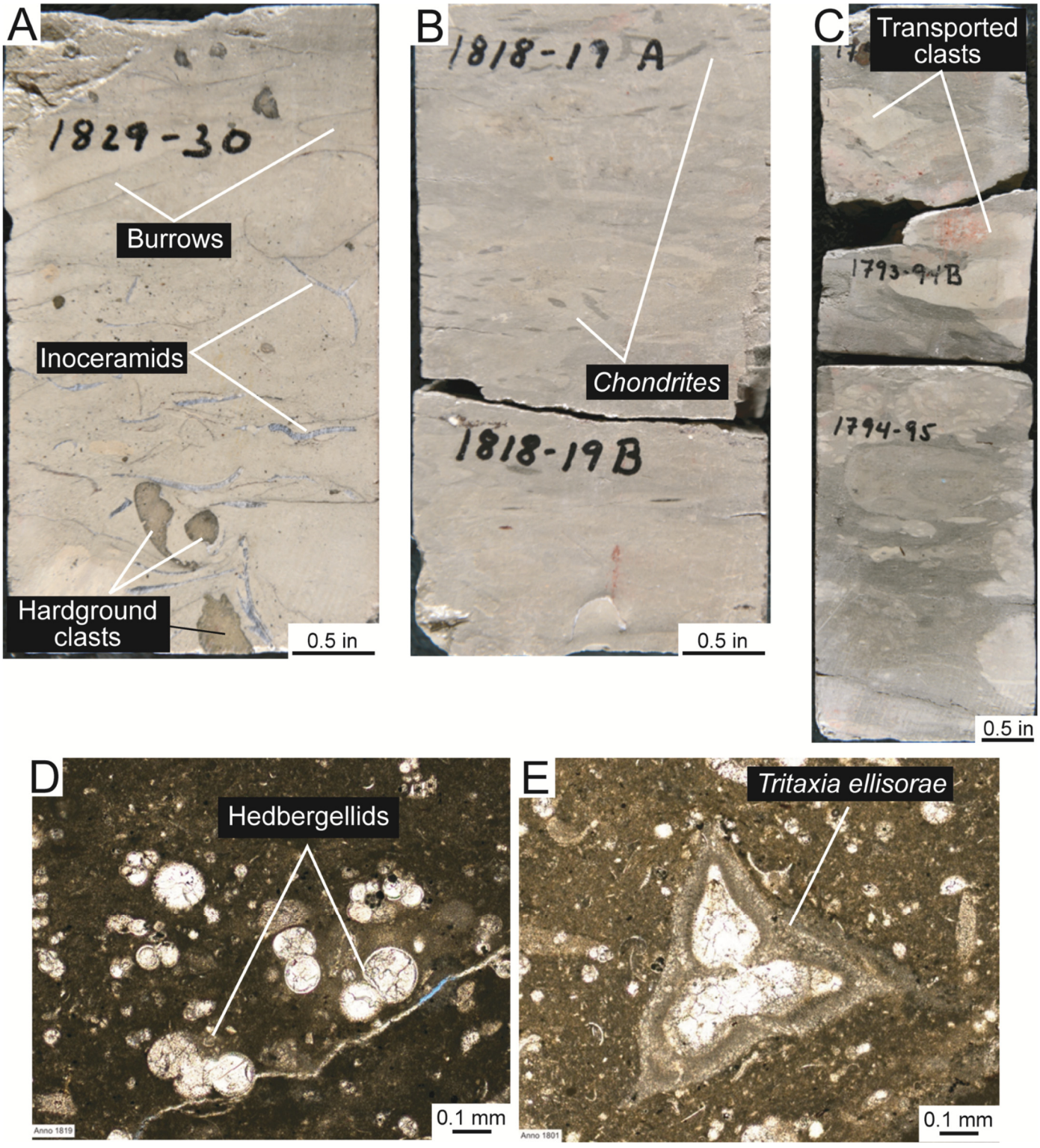

Figure 7. Examples of Ozan lithofacies. (A) 1829 ft: Burrowed lime wackestone with inoceramid fragments and hardground clasts. (B) 1818 ft: Burrowed lime wackestone with *Chondrites* burrows. (C) 1793 ft: Burrowed lime wackestone with transported lime mud clasts. (D) 1819 ft: Wackestone containing globigerinid planktic foraminifers. Matrix showing a peloidal fabric. (E) 1801 ft: Wackestone containing benthic foraminifers.

Marlbrook Chalk

Only 2 ft (0.6 m) of the Marlbrook Chalk was cored (Fig. 4). The samples are similar to those of the Ozan Chalk and Annona Chalk.

Vertical Stratigraphic Trends

The integration of the spontaneous potential (SP) wireline log, core description, and XRF analyses (Fig. 10) shows changes in the vertical trend of calcite and clay content. In this plot, Ca is

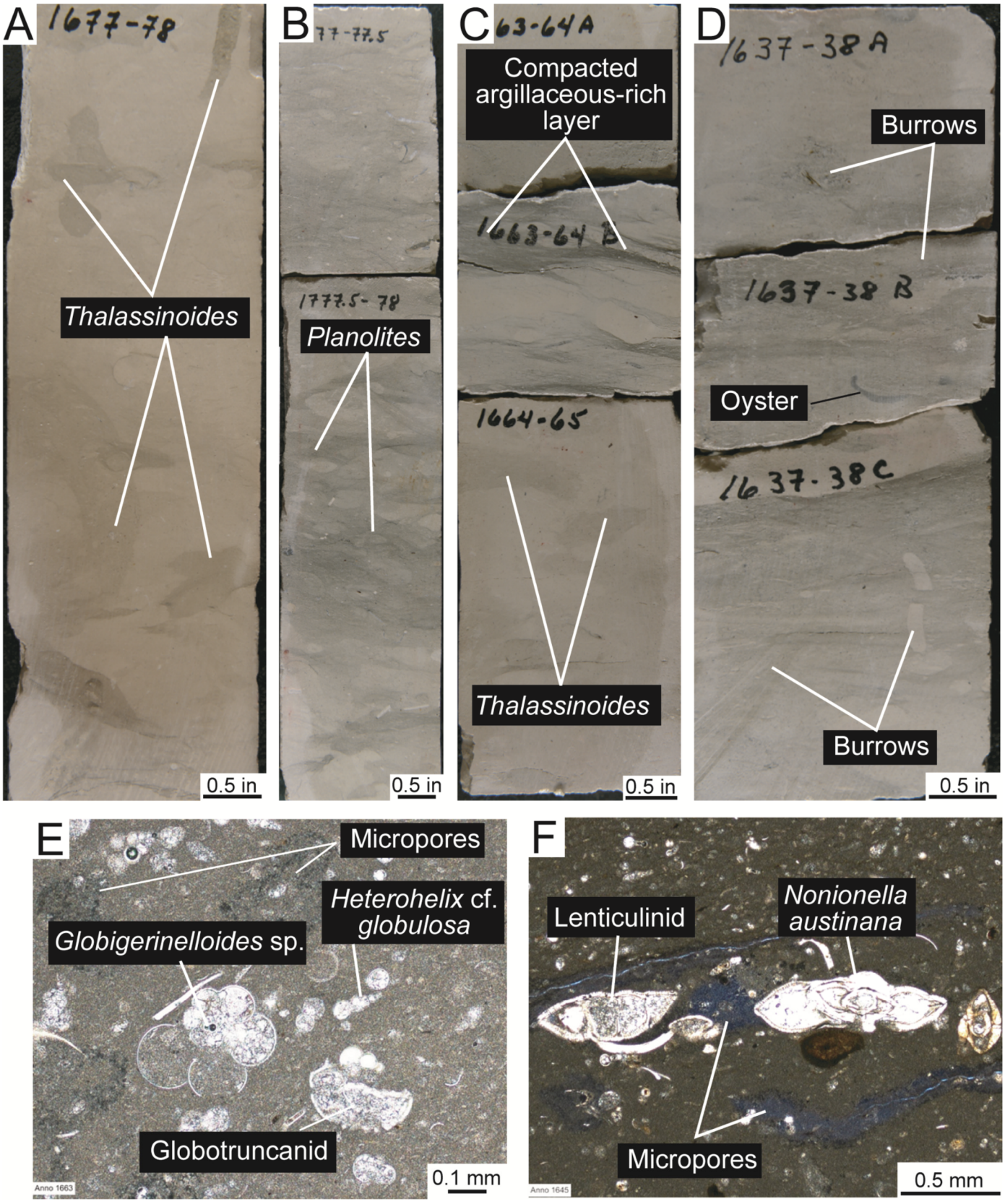

Figure 8. Examples of Annona lithofacies. (A) 1677 ft: Burrowed lime wackestone that is relatively clay free. Some of the burrows are *Thalassinoides*. (B) 1777 ft: Burrowed lime wackestone. Many of the burrows are *Planolites*. (C) 1663 ft: Burrowed lime wackestone with compacted clay-rich seams. (D) 1637 ft: Lime wackestone with argillaceous layers. The blue haze shows microporous areas penetrated by blue fluorescent dyed epoxy. (E) 1663 ft: Lime wackestone with planktic foraminifers. (F) 1646 ft: Peloidal wackestone with benthic foraminifers. The blue haze shows microporous areas penetrated by blue fluorescent dyed epoxy.

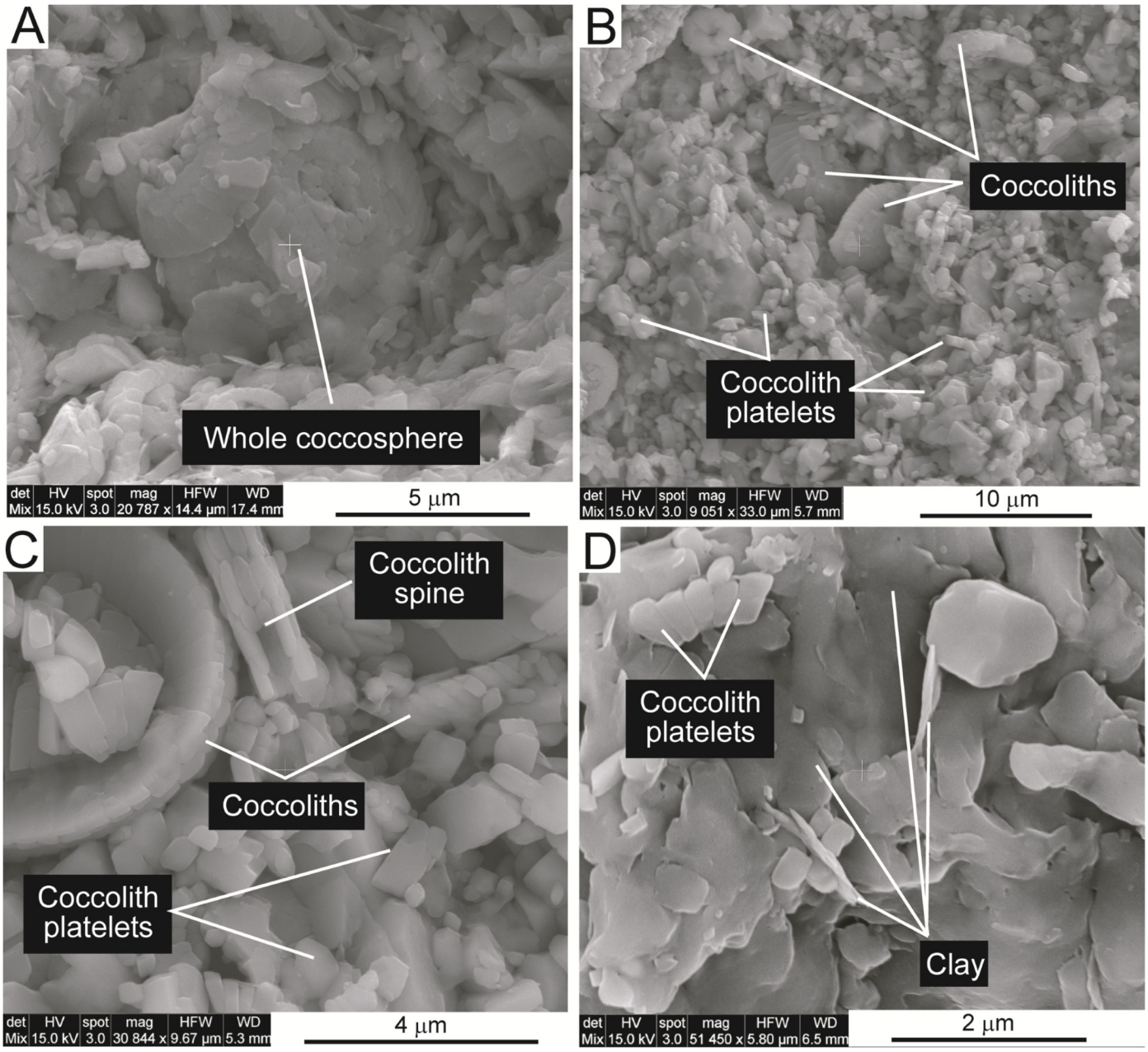

Figure 9. SEM chip examples of matrix. (A) 1770 ft: Whole coccosphere in matrix of coccolith hash. (B) 1675 ft: Chalk matrix composed of coccoliths and coccolith platelets. (C) 1675 ft: Matrix showing coccoliths, coccolith spine, and coccolith platelets. (D) 1711 ft: Matrix mixture of coccolith platelets and clay mineral flakes.

a proxy for calcite, and Al and Ti are proxies for terrigenous input of clay minerals (Rowe et al., 2012). Two vertical trends are noted as a vertical increase in calcite and an associated decrease in clay minerals (Fig. 10).

These repeatable trends, or cycles, can be interpreted as the decrease and increase in terrigenous influx, assuming the calcite production rate by coccoliths and planktic foraminifers remained relatively constant. An increase in terrigenous material may be related to a lowering of sea level, to a regressive part of a cycle, or to a climatic change where more humid conditions with increased rainfall promoted more weathering (increase in clay production) and increased runoff (e.g., Locklair and Sageman, 2008).

DEPOSITIONAL SETTING AND DEPOSITIONAL MODEL

The depositional setting for the Ozan Chalk and Annona Chalk is interpreted to be on a drowned shelf, distal from any siliciclastic source, below storm-wave base, generally low energy, and well oxygenated. Evidence for this interpretation is provided below. Based on the present storm-wave base in the Gulf of Mexico (Reading and Collinson, 1996), the storm-wave base on the Campanian Gulf of Mexico shelf would be expected to be greater than 150 ft (50 m). Bottjer (1981) suggested that the Annona Chalk in southwestern Arkansas to the north of the Caddo–Pine Island Field was deposited in an outer-shelf setting where

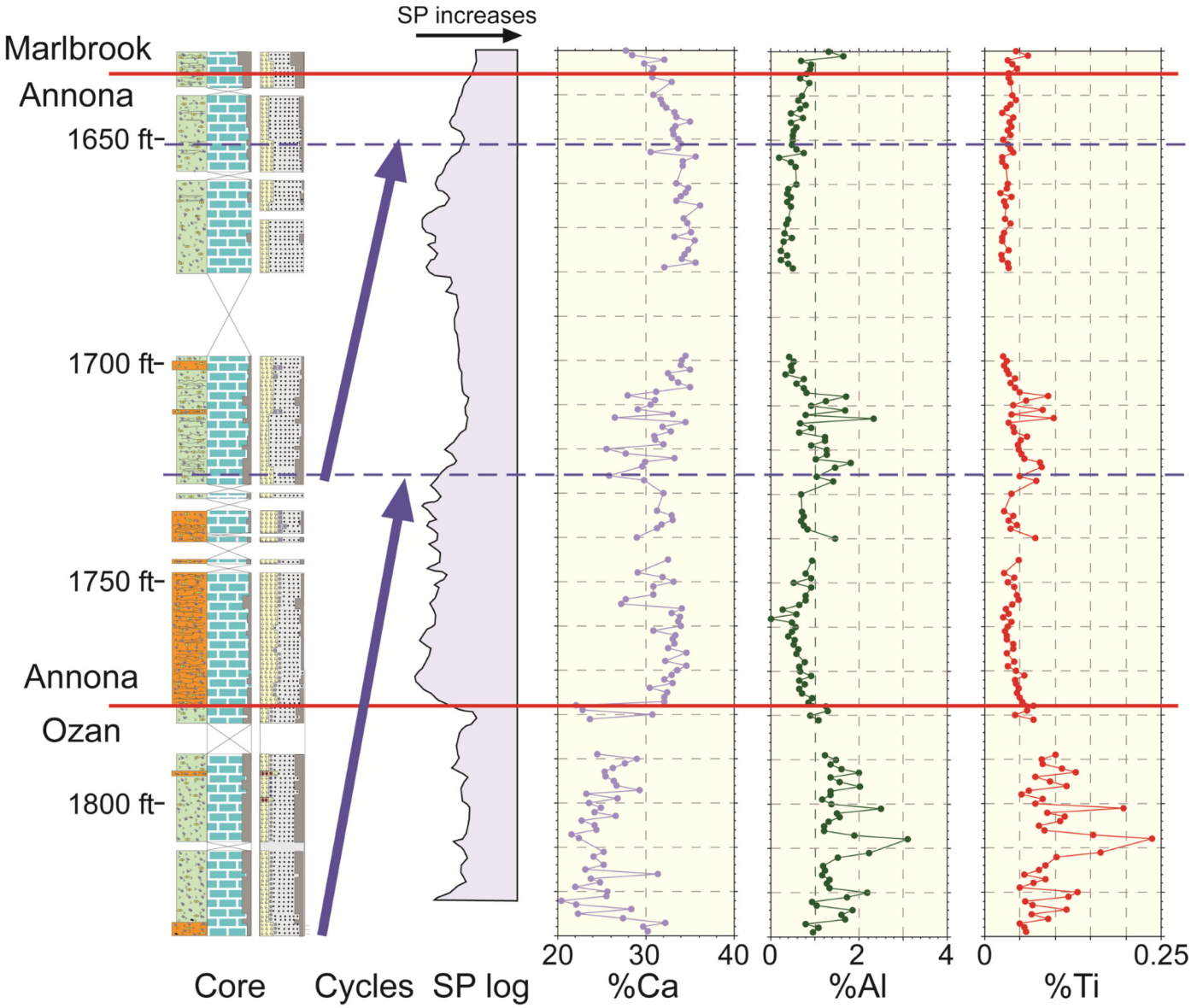

Figure 10. Integration of XRF, SP log, and core data. Ca can be used as a carbonate production proxy, and Al and Ti can be used as a terrigenous input proxy. The graphs show two general upward trends of an increase in Ca (cycles highlighted by blue arrows) and a decrease in Al and Ti. See Figure 4C for core legend.

water depths were between 250 and 400 ft (75 and 125 m). Bottjer (1981) also noted that the flat form of *Zoophycos* might indicate water depths as much as 650 ft (200 m). The major depositional processes in this setting would be suspension settling of biota that lived in the shallow part of the deepwater column, bottom currents generated by storm-return currents, eolian dust clouds, and hemipelagic plumes.

Figure 11 is a two-dimensional model depicting the depositional setting and processes of the Ozan Chalk and Annona Chalk. A deeper-water setting below storm-wave base is based on planktic fauna (including ammonoids, coccospheres, and planktic foraminifers), no preserved hydrodynamic sedimentary structures, and *Chondrites* and *Zoophycos* burrows. Inoceramids also suggests a deeper-water, soupy-sediment setting. Bottjer (1981) recognized that the macroinvertebrates in the Annona show adaption for coping with soft substrates. The deep burrower *Thalassinoides* indicates that both the bottom-water column and the sediment were oxygenated. Organisms will generally not burrow deeply into anoxic sediment (Potter et al., 2005, their figure 4.5).

The siliciclastic material is considered to have been transported into the area of deposition by wind, hemipelagic mud plumes, and storm-return currents. Extensive bioturbation has mixed the siliciclastic material into the carbonate mud. Some of the burrow fills are siliciclastic-rich, indicating the filling of open burrows by storm-return currents. Suspension sedimentation was aided by shallower water-column material flocculating into marine-snow aggregates (e.g., Riebesell, 1992) composed of organic matter, small allochems, and other clay-sized material. The flocculation into aggregates allows rapid settling (Shanks and Trent, 1980). The faint compacted peloids seen in thin section may be this marine snow. The peloids may also be fecal pellets produced by such organisms as copepods (common in the Upper Cretaceous Niobrara Chalk) that lived in the water column (Hattin, 1975; Longman et al., 1998; Loucks and Rowe, 2014).

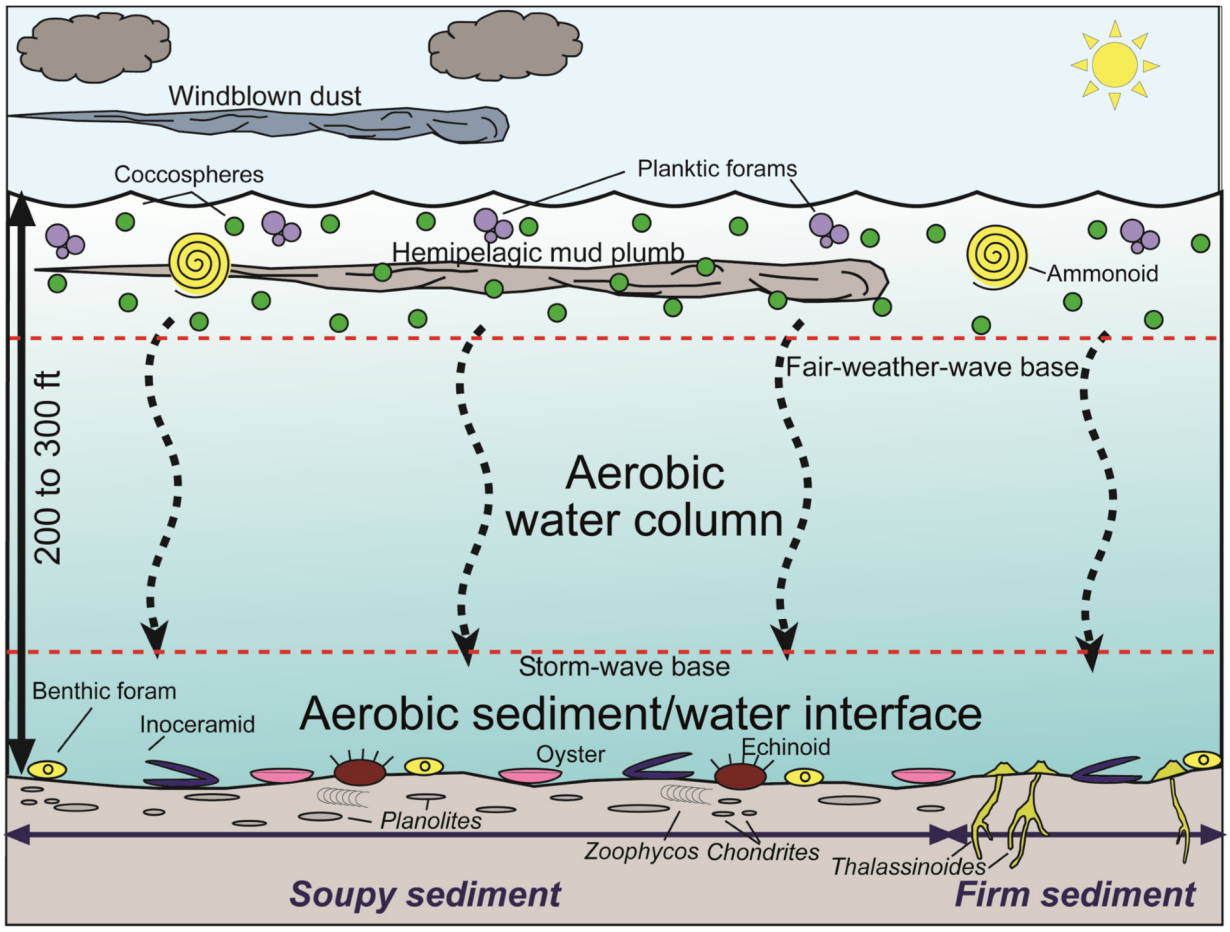

Figure 11. Depositional model for the Annona and Ozan chalks.

DIAGENESIS OF THE OZAN AND ANNONA CHALKS

The diagenesis of chalks is relatively simple because the mineralogy of most of the allochems was low-Mg–calcite (Scholle, 1977a; Hardman, 1982; Fabricius, 2007). Calcite, a relatively stable mineral, commonly does not dissolve readily during diagenesis (Land, 1967). Also, chalks, being deposited in relatively deeper water (several hundreds of feet), are not usually exposed to meteoric water during sea-level drops or early uplift, but rather take a diagenetic pathway directly into the subsurface and remains saturated in a marine brine (e.g., Loucks and Rowe, 2014). Clay minerals (>5%) affect chalk diagenesis during burial (Hardman, 1982); with the Ozan/Annona section having generally more than 5% clay, this clay effect is apparent as discussed below.

An early diagenetic process in coccosphere-rich sediment occurs when the polysaccharide mucus film (bioadhesive) that holds the coccolith plates together (Fabricius, 2007; Jaya et al., 2016) starts to break down, thus allowing the coccoliths to separate into their individual elements (Fabricius, 2007). Bioturbation aids in this breakdown and segmentation. Overall, this process decreases the grain size of these very fine grained sediments from microns in size to submicron in size (Fig. 9).

The major diagenetic process in unlithified chalks is burial compaction (Scholle, 1977a; Fabricius, 2007). At the surface, modern chalk sediment has 67 to 70% porosity (Schlanger and Douglas, 1974; Hamilton, 1976; Scholle, 1977a; Fabricius, 2007). According to Schlanger and Douglas (1974), Hamilton (1976), and Scholle (1977a), by 1500 to 2000 ft (460 to 610 m) of burial of pure chalk, porosity decreases to 45 to 50%. This is far higher than what is recorded in the Ozan (arithmetic mean =17.4%) and Annona (arithmetic mean = 23.8%) chalks.

Two major reasons for this discrepancy may be the Ozan/Annona section was buried much deeper than it is today, or that the clay content has enhanced diagenesis. According to the Scholle compaction curve for chalks (Scholle, 1977a), the Ozan/Annona section would have to have been buried to approximately 5500 to 6000 ft (1675 to 1830 m), a depth not reasonable for the geologic setting of the Ozan Chalk and Annona Chalk in northern Louisiana. A series of burial curves for northern Louisiana constructed by Pitman and Rowan (2012) do not show uplift for the Upper Cretaceous section. Therefore, burial to depths of 5500 to 6000 ft (1675 to 1830 m) are not reasonable and cannot be the cause of the relatively low porosities in the Ozan Chalk and Annona Chalk.

The amount of clay minerals in the Ozan/Annona section (up to 10%) may have affected diagenesis by promoting compaction and dissolution of the carbonate and reprecipitation of the carbonate as calcite cement. Hardman (1982) concluded that clay mixed within coccolith-rich sediments rotates during burial and enhances compaction. He stated that early extensive lithification is generally not seen in argillaceous chalks. The lack of cementation would allow greater compaction before a rigid framework was established.

At some depth of burial—depending on time, temperature, pressure, and clay-mineral content—the coccolith and coccolith elements begin to cement together. Figure 12 shows the general procedure for cementation of the coccoliths and coccolith platelets. According to Fabricius (2007), the source of carbonate for cementation is burial dissolution of the coccolith elements by pressure dissolution at the clay-calcite interface. The coccoliths

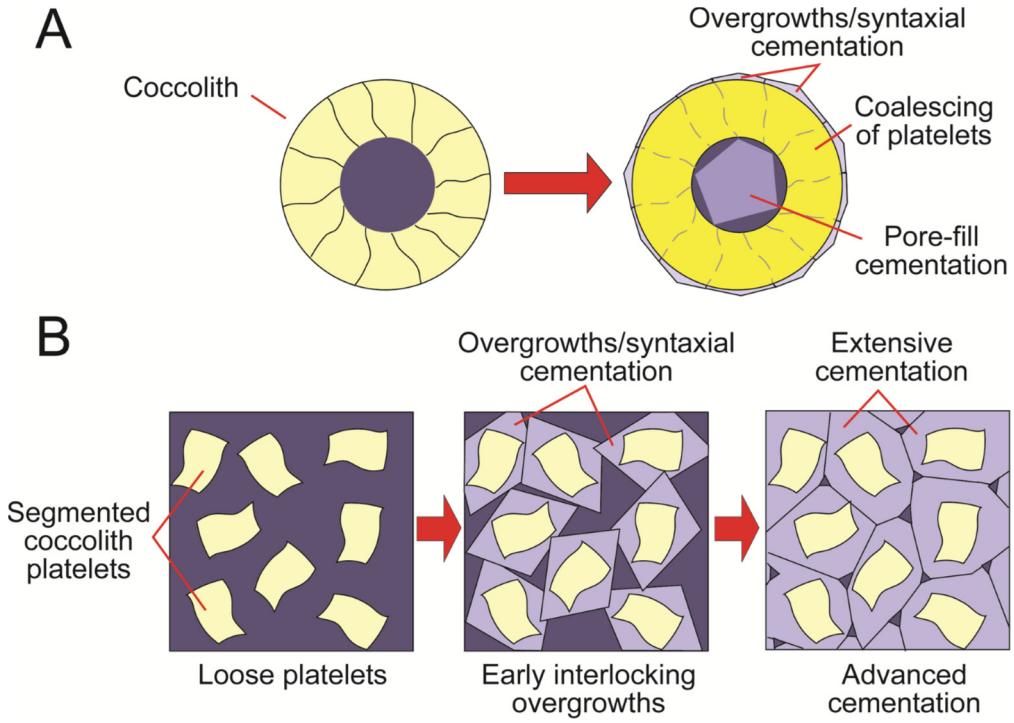

Figure 12. Chalk diagenesis diagrams. (A) Cementation of a coccolith. (B) Cementation of coccolith platelets.

that are still intact will be cemented together by calcite cement (Fig. 12A). The in-place platelets will fuse together (Figs. 13B and 13C), and calcite syntaxial overgrowths will form on the platelets. Also, calcite crystals form in the center of the coccolith plate (Fig. 14A). Calcite cement will also begin to grow around the disaggregated platelets. As this cementation process progresses, the cement will weld the coccoliths and platelets into a lithified rock (Figs. 13–15). The amount of porosity that remains depends on the degree of compaction and the amount of cementation.

RESERVOIR QUALITY

Reservoir quality is a function of dimensions of the reservoir, heterogeneity (continuity and variability), porosity, and permeability. At the reservoir scale, chalks are deposited on shelves in generally deepwater, which leads to relatively uniform depositional conditions resulting in good continuity and low variability; at the finer scale, however, this may not be the case (Frébourg et al., 2016). This section on reservoir quality will concentrate on the origin, type, and abundance of pores (porosity) and associated permeability.

Reservoir quality of other chalks has been addressed in many studies (e.g., Scholle, 1977a; Hardman, 1982; Fabricius, 2007; Loucks and Rowe, 2014; Loucks and Gates, 2015). As noted earlier, published plots of porosity versus depth have been presented by several authors (e.g., Schlanger and Douglas, 1974; Hamilton, 1976; Scholle, 1977a). There are also some published plots addressing permeability versus depth (e.g., Mallon et al., 2005). It needs to be noted that fractures can be the prominent flow system in chalk reservoirs, as seen in the Buda and Austin Chalk plays (Scholle, 1977b). In the investigated core, no fractures were noted.

The Ozan Chalk and Annona Chalk are argillaceous, as noted earlier, and appear to have undergone rapid porosity and permeability loss. The characterization of pore types and methods of porosity lost is addressed using thin sections, SEM chips and Ar–ion milled samples, and MICP analyses. Each method addresses different characteristics of the pore network. Thin sections present data on the millimeter- to centimeter-scale pore network, SEM observations provide data at the nanometer to micrometer scale on pore types and associated diagenesis, and MICP analysis characterizes pore-throat-size distribution.

Pore Types, Pore Throats, and Pore Network

Analysis of thin sections indicates no macropores (>10 microns); the only pores visible are nano- and micropores. Nano- and micropore distribution as shown in thin sections under UV light is patchy to continuous (Fig. 16). All nano- and micropores are in the matrix, except for a minor amount of intraparticle micropores within partially cemented body cavities of planktic foraminifers (Figs. 13–15). The cause of patchiness of pore distribution in the mud matrix is not obvious but may be related to resedimented compacted peloids and soft clasts that commonly have a different grain-packing arrangement than that of the regular mud matrix. It has been well documented that resedimented muds in chalks can have a different packing arrangement and higher porosities (Fabricius, 2007; Loucks and Gates, 2015). Also, the patchiness could be related to indistinct bioturbation.

SEM imaging of Ar–ion-milled samples of the chalks (Figs. 13–15) allows for detailed analysis of pores. The samples display a pore network of nano- to micropores. Interparticle pores lie between the coccolith platelets, and intraparticle pores occur within planktic foraminifers. Pores in the matrix are generally smaller than a micron, but some are as large as 2 microns (Figs. 14 and 15). The larger pores—some as large as 4 to 5 microns—lie within the planktic foraminifers (Figs. 13–15). The larger pores in the body cavities are related to how much debris is introduced into the body cavity or how much cementation has occurred. Some planktic foraminifer bodies are as large as 60 microns, as shown in Figure 13A. In this intraparticle pore, some coccolith platelet debris was introduced and cementation occurred, transforming a simple, larger intraparticle pore into a number of smaller intraparticle pores. Another type of intraparticle pore is shown in Figure 14D. The original Mg–calcite test has transformed to calcite, forming microrhombic and associated nanopores, a process documented by Loucks et al. (2013).

Figure 13 shows small-scale distribution of pores. In Figure 13A, the pores are composed of interparticle nano- to mi-

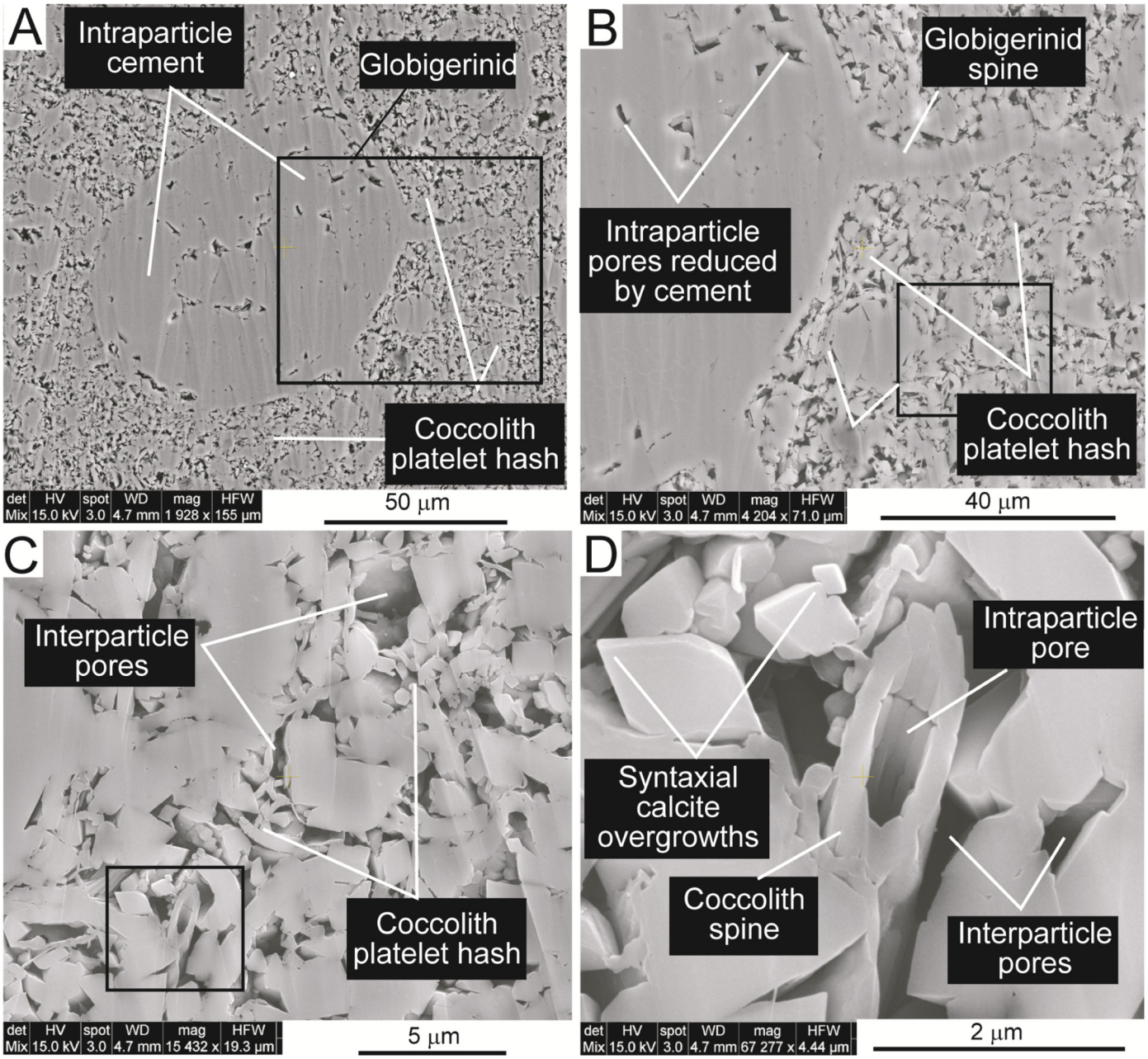

Figure 13. Pore networks. All images from Ar–ion-milled stubs. (A) 1827 ft: Globigerinid with spines immersed in coccolith hash containing abundant interparticle pores. Globigerinid has cement-reduced intraparticle pores. (B) 1827 ft: Same as A but closer view. (C) 1827 ft: Same as A and B but closer view showing coccolith platelets. (D) 1827 ft: Same as A, B, and C but greatly enlarged, showing coccolith platelets and spine. Some platelets show rhombic calcite cement overgrowths.

cropores within the coccolith and coccolith-platelet matrix. Micron-sized pores occur within the foraminifer grains as cement-reduced intraparticle pores. Figures 13B and 13C show the same sample at higher magnifications. The interparticle pores between the coccolith platelets are well displayed in Figure 13C.

Core-plug porosity and permeability are displayed in Figure 17. Porosities are fair for the Ozan Chalk and very good for the Annona Chalk, but the associated permeabilities are poor. Arithmetic mean porosity for the Annona Chalk is 23.8% and arithmetic mean permeability is 0.42 md. For the Ozan Chalk, arithmetic mean porosity is 17.4% and arithmetic mean permeability is 0.19 md. The lower reservoir quality for the Ozan Chalk is related to the relatively higher clay-mineral content, as shown by the XRF analysis (Fig. 10).

MICP analysis was completed on one Ozan Chalk and one Annona Chalk sample (Fig. 18). The Annona sample is very porous (27.2%) and the Ozan sample has fair porosity (15.2%). Figure 18A shows the MICP plots for both samples, with the Annona sample having an entry pressure of approximately 400 psi (2.8 MPa) and the Ozan sample having an entry pressure of approximately 2000 psi (13.8 MPa), indicating the better reservoir quality of the Annona sample. However, both samples actually have poor to very poor permeability (Annona core-plug sample permeability = 0.912 md; Ozan core-plug sample permeability = 0.018 md). The differences in reservoir quality between the two samples and overall reservoir quality of these tight chalks is shown by plots of pore-throat sizes calculated from MICP analyses (Figs. 18C and 18D). Both samples show a well-sorted pore-throat population with all pores in the nano- to micropore

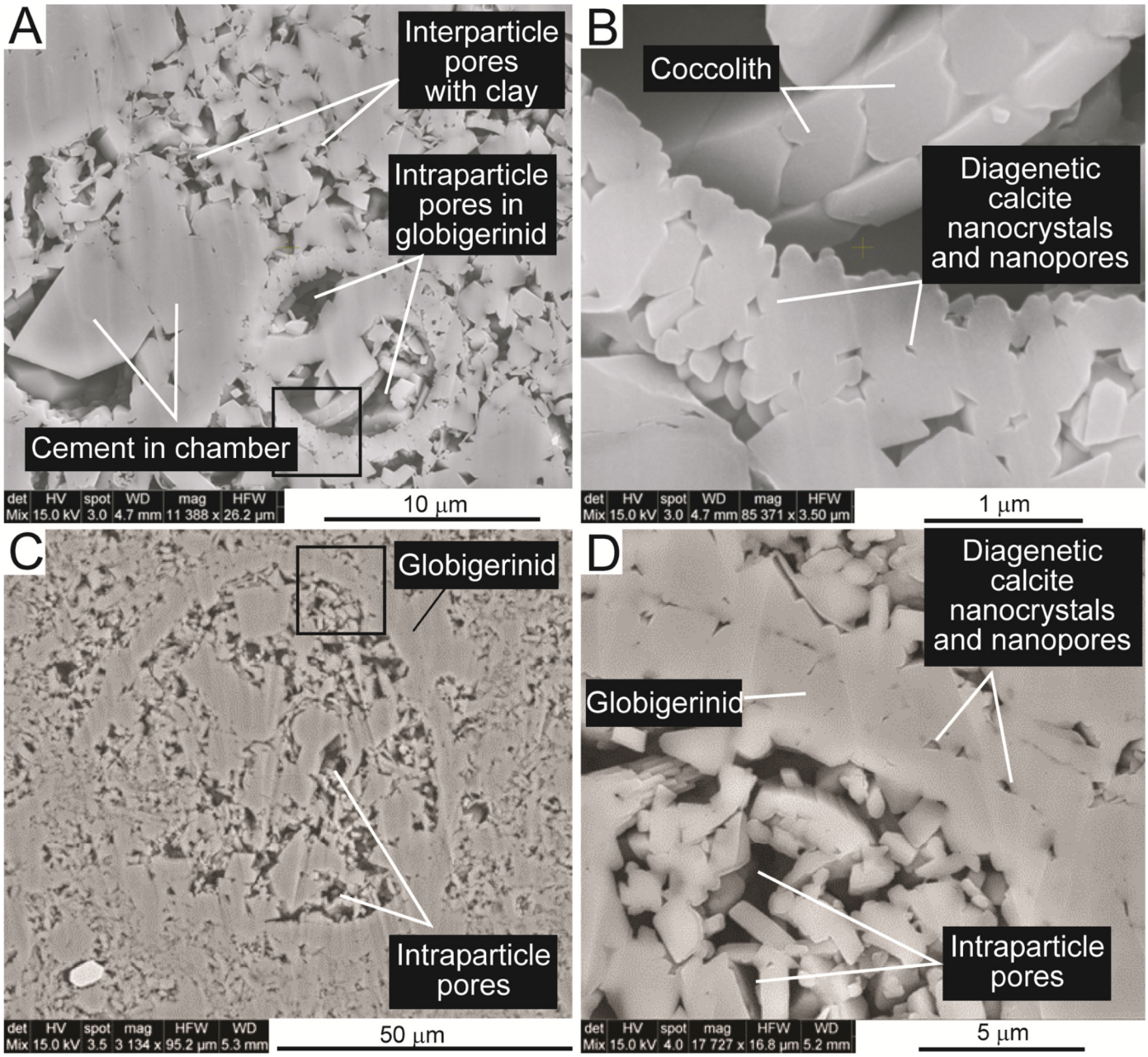

Figure 14. Pore networks. All images from Ar–ion-milled stubs. (A) 1827 ft: Coccolith hash with interparticle and intraparticle nano- and micropores. Some calcite cement crystals in chambers. (B) 1827 ft: Same as A but closer view showing altered wall of foraminifer to nanocrystalline calcite with nanopores. (C) 1675 ft: Globigerinid in coccolith hash. Matrix has abundant interparticle pores and globigerinid has cement-reduced intraparticle pores. (D) 1675 ft: Same as C but closer view of coccolith hash and associated nanopores. Notice that the coccolith hash in the intraparticle pore was sheltered from compaction.

throat range. The Ozan sample has a median pore-throat radius of 0.03 microns, and the Annona sample has a median pore-throat radius of 0.18 microns.

Overall, the pore network in the Annona Chalk and Ozan Chalk is composed of nanopores and micropores connected by very fine pore throats (on average, pore-throat radius is less than 0.2 microns). According to Pittman (1971), these chalks meet the engineering definition of a micropore reservoir because the pore-throat radii are less than 0.5 microns. The pores consist of interparticle pores between coccoliths and coccolith platelets in the matrix, and intraparticle pores within planktic foraminifer. The interparticle pores form the effective pore network, whereas the intraparticle pores contribute to volume but may not add to the effective pore network because they are in relatively isolated domains.

An article on the *Caddo Chalk Formation Times* website (Anonymous, 2011) speculated that the Annona Chalk has massive reserves (no amount given), with the producing zone ranging from 150 to 250 ft (46 to 76 m) in thickness. The article estimates that approximately 6% of total reserves have been produced. The oil is paraffin-based with an American Petroleum Institute (API) gravity of 42 to 44°. At the present time, the wells are considered stripper wells. However, with the advent of horizontal drilling techniques, the Annona may again offer better producing wells (e.g., PR Newswire, 2004).

CONCLUSIONS

The Campanian Annona Chalk and Ozan Chalk were deposited during a second-order sea-level rise on the drowned Lower

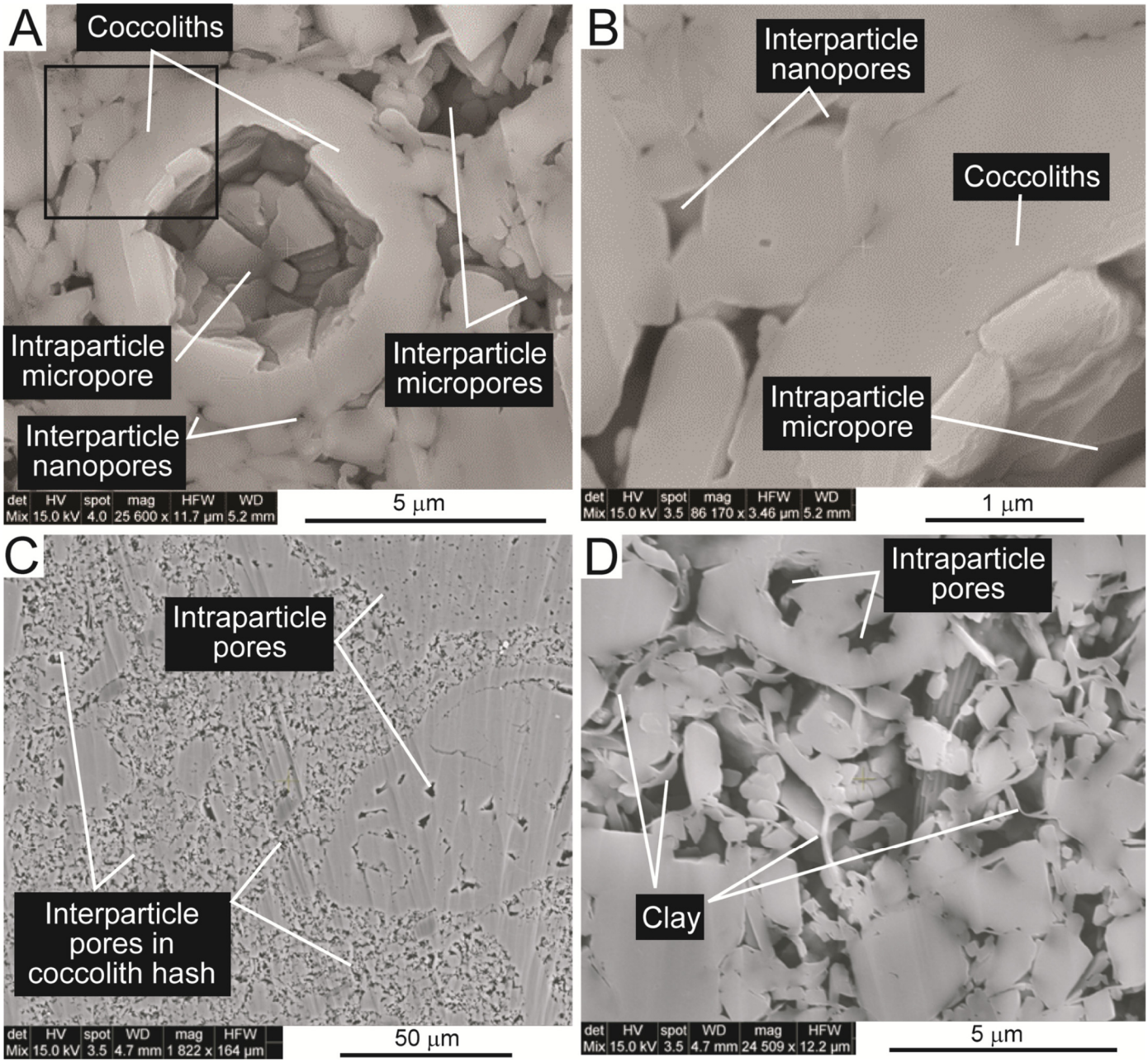

Figure 15. Pore networks. All images from Ar–ion-milled stubs. (A) 1827 ft: Coccolith with large intraparticle pore. (B) 1827 ft: Same as A but closer view. Many pores are in the nanopore range. (C) 1827 ft: Globigerinid with internal calcite cement in a finer matrix of interparticle-rich coccolith hash. (D) 1827 ft: Same as C but closer view. Many of the interparticle pores are reduced in size by clay-mineral flakes.

Cretaceous constructed platform. Depositional setting for these chalks is interpreted as occurring on a drowned shelf, distal from any siliciclastic source; below storm-wave base; and in a low-energy, well-oxygenated environment. Several cycles of covariant calcite and clay-mineral abundance suggest changes either in sea level or climate or a combination of both.

The diagenesis of the chalky marls was relatively simple, with burial compaction and calcite cementation being the primary causes of porosity lost. The outcome of clay-mineral-enhanced compaction and calcite cementation produced tight carbonates. The pore network consists of primary interparticle and intraparticle nano- to micropores. Arithmetic mean porosity for the Annona Chalk is 23.8% and arithmetic mean permeability is 0.42 md. For the Ozan Chalk, arithmetic mean porosity is 17.4% and arithmetic mean permeability is 0.19 md.

The Annona Chalk has been a productive chalk since 1905 and continues to produce to the present. With advanced drilling and completion technologies and an estimated 94% of in-place reserves remaining, this shallowly buried chalk will be of continued economic interest. With a future increase in oil prices, even the Ozan Chalk may become of interest as an oil target.

ACKNOWLEDGMENTS

The authors would like to express their appreciation to the reviewers of this manuscript, Mark Longman and Ryan Phelps; to Barry Katz, *GCAGS Journal* editor; to James J. Willis, GCAGS managing editor; and to Stephanie Jones, the Bureau of Economic Geology editor. This work was completed at the Bureau of Economic Geology Carbonate Reservoir Research Labor-

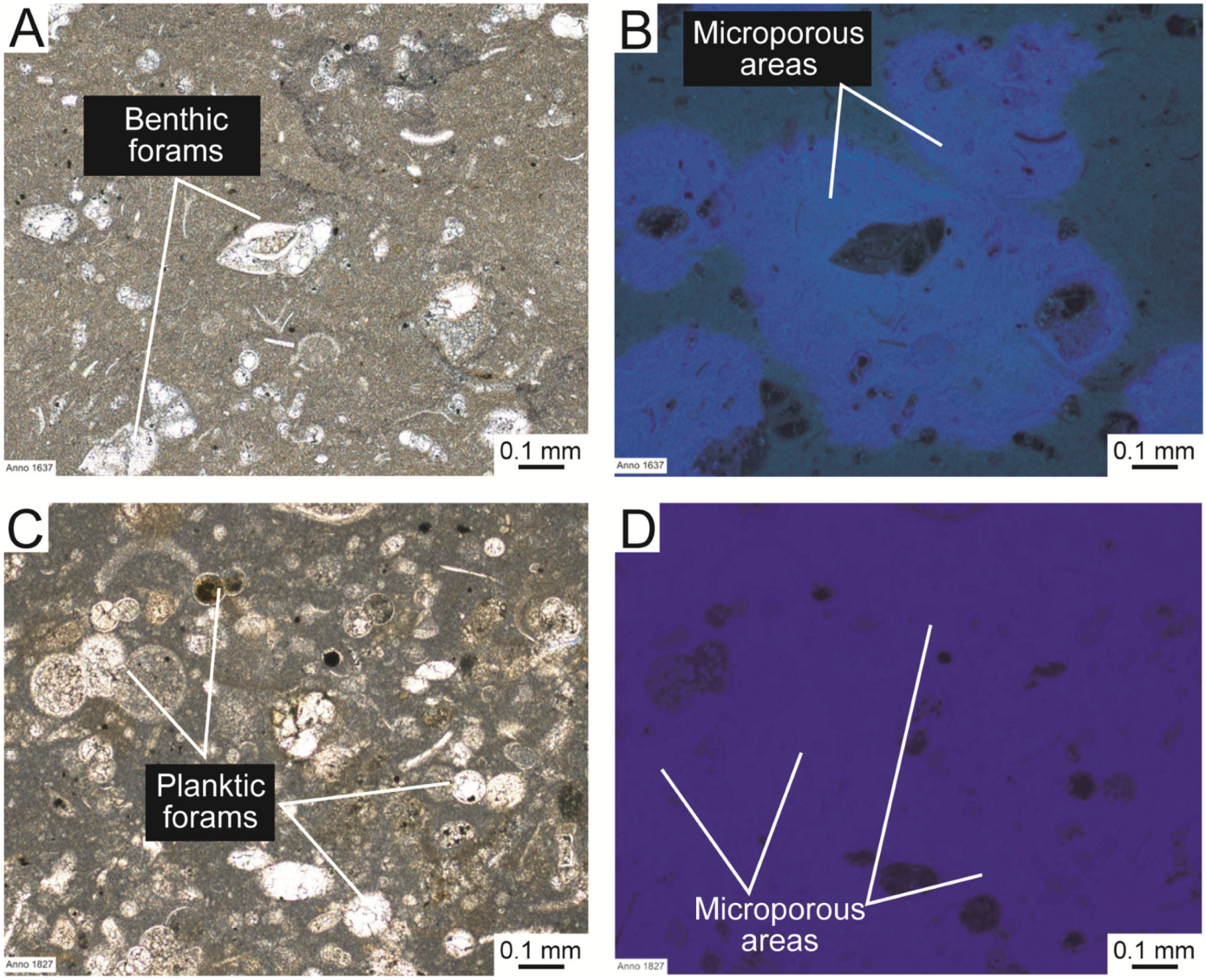

Figure 16. Thin-section examples of nano- and micropore distribution. (A) 1327 ft: Lime wackestone. (B) 1327 ft: Same as A but photo taken with UV light. Porous areas are highlighted in blue. Distribution is patchy and may be related to porous peloids or very small lime mud clasts. (C) 1827 ft: Lime packstone. (D) 1827 ft: Same as C but photo taken with UV light. The fine matrix is porous.

atory (RCRL). We thank Patrick Smith for working with us on the SEM and aiding us in the production of the SEM images. Publication authorized by the Director, Bureau of Economic Geology, Jackson School of Geosciences, University of Texas at Austin.

REFERENCES CITED

Anonymous, 2011, Caddo Pine Island: Caddo Chalk Formation Times, August 21 posting, <http://roseandson.blogspot.com/> Last accessed January 9, 2017.

Blakey, R. C., 2016, Paleogeography and geologic evolution of North America: Images that track the ancient landscapes of North America (Late Cretaceous–75 Ma): Northern Arizona University School of Earth Sciences and Environmental Sustainability, Flagstaff, <http://jan.ucc.nau.edu/rcb7/nam.html> Last accessed January 16, 2017.

Bottjer, D. J., 1981, Structure of Upper Cretaceous chalk benthic communities, southwestern Arkansas: Palaeogeography, Palaeoclimatology, Palaeoecology, v. 34, p. 225–256, doi:10.1016/0031-0182(81)90068-7.

Bottjer, D. J., 1985, Trace fossils and paleoenvironments of two Arkansas Upper Cretaceous discontinuity surfaces: Journal of Paleontology, v. 59, p. 282–298, <http://www.jstor.org/stable/1305028> Last accessed June 13, 2017.

Crane, M. J., 1965, Upper Cretaceous ostracodes of the Gulf Coast area: Micropaleontology, v. 11, p. 191–254, doi:10.2307/1484517.

Cushing, E. M., E. H. Boswell, and R. L. Hosman, 1964, General geology of the Mississippi Embayment: Water resources of the Mississippian Embayment: U.S. Geological Survey Professional Paper 448–B, p. B1–B28, <https://pubs.usgs.gov/pp/0448b/report.pdf> Last accessed June 13, 2017.

Dunham, R. J., 1962, Classification of carbonate rocks according to depositional texture, *in* W. E. Ham, ed., Classification of carbonate rocks: American Association of Petroleum Geologists Memoir 1, Tulsa, Oklahoma, p. 108–121.

Fabricius, I. L., 2007, Chalk: Composition, diagenesis and physical properties: Bulletin of the Geological Society of Denmark, v. 55, p. 97–128, <http://orbit.dtu.dk/files/3077185/Side%2097-128.pdf> Last accessed June 13, 2017.

Frébourg, G., S. C. Ruppel, R. G. Loucks, and J. Lambert, 2016, Depositional controls on sediment body architecture in the

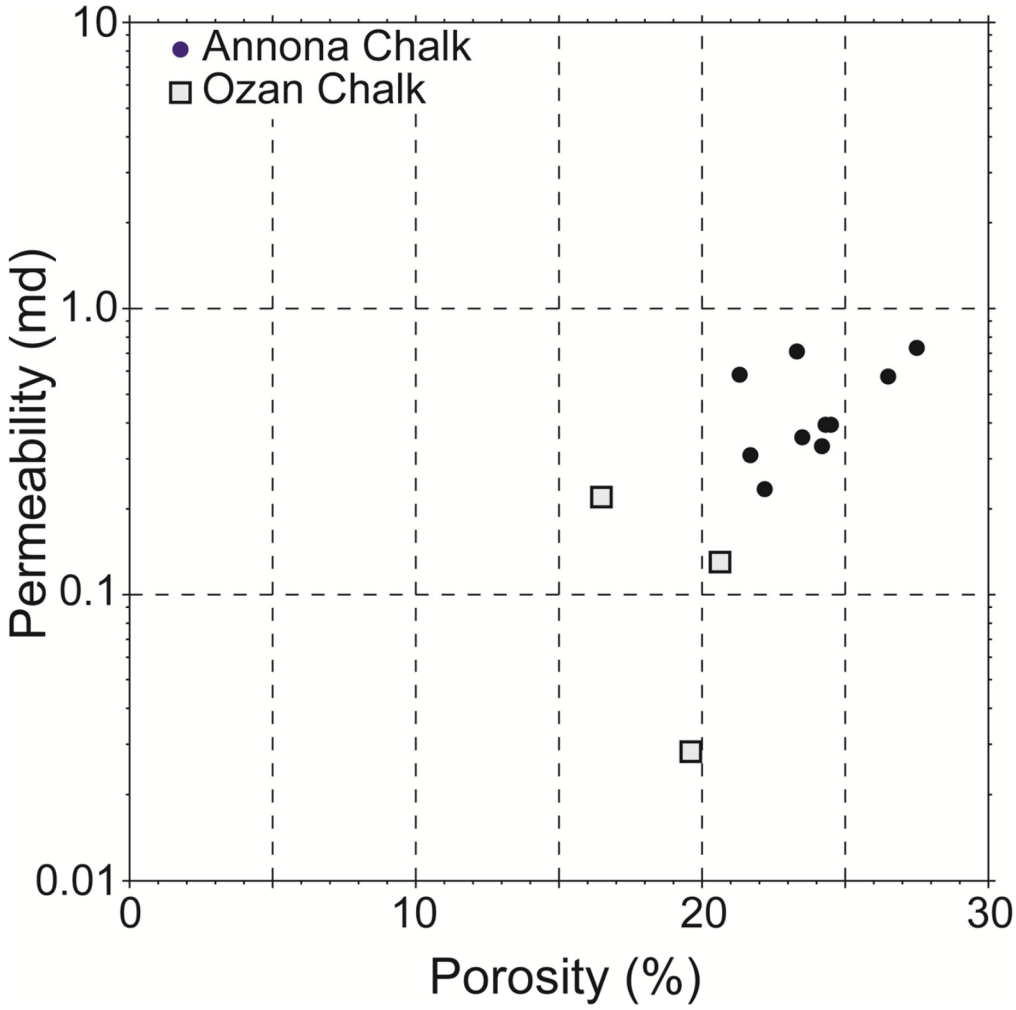

Figure 17. Porosity versus permeability plot.

Eagle Ford/Boquillas system: Insights from outcrops in West Texas, United States: American Association of Petroleum Geologists Bulletin, v. 100, p. 657–682, doi:10.1306/12091515101.

Hamilton, E. L., 1976, Variations of density and porosity with depth in deep-sea sediments: Journal of Sedimentary Petrology, v. 46, p. 280–300, doi:10.1306/212f6f3c-2b24-11d7-8648000102c1865d.

Hardman, R. F. P., 1982, Chalk reservoirs of the North Sea: Bulletin of the Geological Society of Denmark, v. 30, p. 119–137, <https://2dgf.dk/xpdf/bull30-03-04-119-137.pdf> Last accessed June 13, 2017.

Hattin, D. E., 1975, Petrology and origin of fecal pellets in upper Cretaceous strata of Kansas and Saskatchewan: Journal of Sedimentary Research, v. 45, p. 686–696, doi:10.1306/212f6e10-2b24-11d7-8648000102c1865d.

Jaya, B. N., R. Hoffman, C. Kirchlechner, G. Dehm, C. Scheu, and G. Langer, 2016, Coccospheres confer mechanical protection: New evidence for an old hypothesis: *Acta Biomaterialia*, v. 42, p. 258–264, doi:10.1016/j.actbio.2016.07.036.

Johnston, III, J. E., P. V. Heinrich, J. K. Lovelace, R. P. McCulloh, and R. K. Simmerman, 2000, Stratigraphic charts of Louisiana: Louisiana Geological Survey Folio Series 8, Baton Rouge, 6 p.

Kennedy, W. J., and R. E. Garrison, 1975, Morphology and genesis of nodular chalks and hardgrounds in the Upper Cretaceous of southern England: Sedimentology, v. 22, p. 311–386, doi:10.1111/j.1365-3091.1975.tb01637.x.

Land, L. S., 1967, Diagenesis of skeletal carbonates: Journal of Sedimentary Research, v. 37, p. 914–930, doi:10.1306/74d717d5-2b21-11d7-8648000102c1865d.

Locklair, R. E., and B. B. Sageman, 2008, Cyclostratigraphy of the Upper Cretaceous Niobrara Formation, Western Interior, U.S.A.: A Coniacian-Santonian orbital timescale: Earth and Planetary Science Letters, v. 269, p. 540–553, doi:10.016/j.epsl.2008.03.021.

Longman, M. W., B. A. Luneau, and S. M. Landon, 1998, Nature and distribution of Niobrara lithologies in the Cretaceous western interior of the Rocky Mountain region: The Mountain Geologist, v. 35, no. 4, p. 137–170.

Loucks, R. G., and B. Gates, 2015, Nanopore and fracture duel pore network in the Upper Cretaceous Buda Formation, Dimmit Co., Texas (abs.): American Association of Petroleum Geologists Search and Discovery Article 90216, Tulsa, Oklahoma, <http://www.searchanddiscovery.com/abstracts/html/2015/90216ace/abstracts/2097581.html> Last accessed June 13, 2017.

Loucks, R. G., F. J. Lucia, and L. E. Waite, 2013, Origin and description of the micropore network within the Lower Cretaceous Stuart City Trend tight-gas limestone reservoir in Pawnee Field in South Texas: Gulf Coast Association of Geological Societies Journal, v. 2, p. 29–41, <http://www.gcags.org/Journal/2013.gcags.journal/GCAGS.Journal.2013.vol2.p29-41.Loucks.et.al.pdf> Last accessed June 13, 2017.

Loucks, R. G., R. M. Reed, S. C. Ruppel, and D. M. Jarvie, 2009, Morphology, genesis, and distribution of nanometer-scale pores in siliceous mudstones of the Mississippian Barnett Shale: Journal of Sedimentary Research, v. 79, doi:10.2110/jsr.2009.092.

Loucks, R. G., and H. D. Rowe, 2014, Upper Cretaceous Niobrara Chalk in Buck Peak Field, Sand Wash Basin, NW Colorado: Depositional setting, lithofacies, and nanopore network:

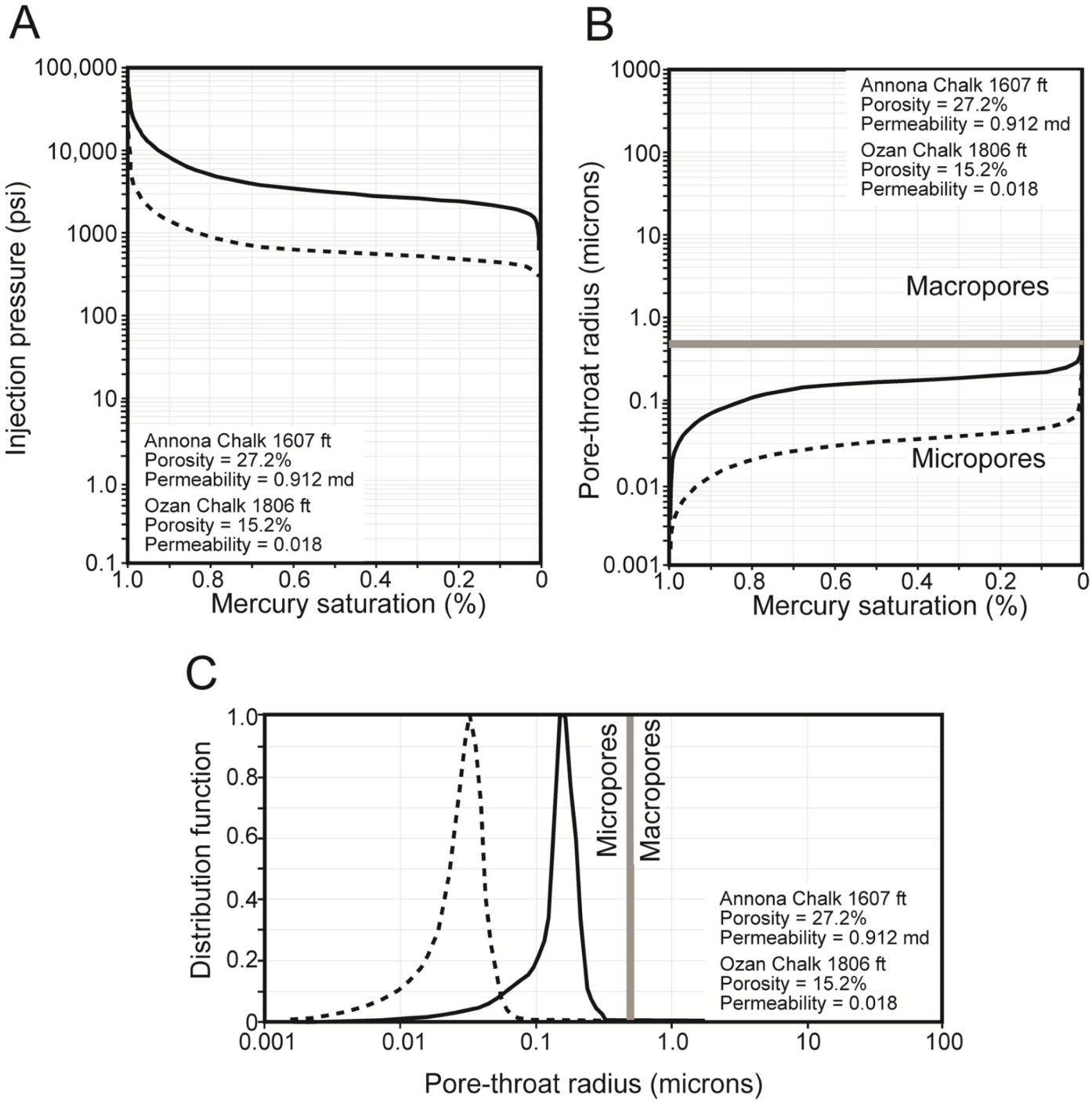

Figure 18. Mercury-injection capillary-pressure data. (A) Mercury saturation versus injection pressure. High injection pressures are associated with low permeabilities. (B) Mercury saturation versus pore-throat size. All pore throats are in the nano- to micropore size range. (C) Pore-throat-radius distribution curves.

Unconventional Resources Technology Conference Paper 1918913, Denver, Colorado, 13 p., doi:10.15530/urtec-2014-1918913.

Mallon, A. J., R. E. Swarbrick, and T. J. Katsube, 2005, Permeability of fine-grained rocks: New evidence from chalks: Geology, v. 33, p. 21–24, doi:10.1130/g20951.1.

Phelps, R. M., C. Kerans, R. G. Loucks, R. O. B. P. Da Gama, J. Jeremiah, and D. Hull, 2014, Oceanographic and eustatic control of carbonate platform evolution and sequence stratigraphy on the Cretaceous (Valanginian-Campanian) passive margin, northern Gulf of Mexico: Sedimentology, v. 61, p. 461–496, doi:10.1111/sed.12062.

Pitman, J. K., and E. Rowan, 2012, Temperature and petroleum generation history of the Wilcox Formation, Louisiana: U.S. Geological Survey Open-File Report 2012–1046, 51 p., <https://pubs.usgs.gov/of/2012/1046/report/OF12-1046.pdf> Last accessed June 13, 2017.

Pittman, E. D., 1971, Microporosity in carbonate rocks: American Association of Petroleum Geologists Bulletin, v. 55, p. 1873–1881, doi:10.1306/819a3db2-16c5-11d7-8645000102c1865d.

Potter, P. E., J. B. Maynard, and P. J. Depetris, eds., 2005, Mud and mudstones: Springer Science & Business Media, Berlin/Heidelberg, Germany, 297 p., doi:10.2113/100.7.1469.

PR Newswire, 2004, Metro Energy reports second well success using Verdisys Technology, <http://www.prnewswire.com/news-releases/metro-energy-reports-second-well-success-using-verdisys-technology-74142522.html> Last accessed January 9, 2017.

Reading, H. G., and J. D. Collinson, 1996, Clastic coasts, *in* H. G., Reading, ed., Sedimentary environments: Processes, facies and stratigraphy: Blackwell Science, Oxford, U.K., p. 154–258.

Riebesell, U., 1992, The formation of large marine snow and its sustained residence in surface waters: Limnology and Oceanography Letters, v. 37, p. 63–76, doi:10.4319/lo.1992.37.1.0063.

Rowe, H. D., N. Hughes, and K. Robinson, 2012, The quantification and application of handheld energy-dispersive X–ray fluorescence (ED–XRF) in mudrock chemostratigraphy and geochemistry: Chemical Geology, v. 324–325, p. 122–131, doi:10.1016/j.chemgeo.2011.12.023.

Sartor, C. L., 2003, Early history of the Caddo–Pine Island Field: Oil-Industry History, Petroleum History Institute, v. 4, p. 3–12. Abstract available at <http://petroleumhistory.org/oil-industry-history/volume-4/> Last accessed June 13, 2017.

Schlanger, S. O., and R. G. Douglas, 1974. The pelagic ooze-chalk-limestone transition and its implications for marine stratigraphy, *in* K. J. Hsü and H. C. Jenkyns, eds., Pelagic sediments: On land and under the sea: International Association of Sedimentology Special Publication 1, Gent, Belgium, p. 117–148, doi:10.1002/9781444304855.ch6.

Scholle, P. A., 1977a, Chalk diagenesis and its relationship to petroleum exploration: Oil from chalks, a modern miracle?: American Association of Petroleum Geologists Bulletin, v. 61, p. 982–1009, doi:10.1306/c1ea43b5-16c9-11d7-8645000102c1865d.

Scholle, P. A., 1977b, Current oil and gas production from North American Upper Cretaceous Chalks: U. S. Geological Survey Circular 767, 51 p., <https://pubs.usgs.gov/circ/1977/0767/report.pdf> Last accessed June 13, 2017.

Shanks, A. L., and J. D. Trent, 1980. Marine snow: Sinking rates and potential role in vertical flux: Deep-Sea Research, v. 27, p. 137–143, doi:10.1016/0198-0149(80)90092-8.

Thomas, N. L., and E. M. Rice, 1932, Notes on the Annona Chalk: Journal of Paleontology, v. 6, p. 319–329, <http://www.jstor.org/stable/1298209> Last accessed June 13, 2017.